Oxychloridoselenites(IV) with Cuban-Derived Anions and Step-Wise Chlorine-to-Oxygen Exchange

Maxime A. Bonnin[a] and Claus Feldmann[a]*

[a]Institute of Inorganic Chemistry (IAC), Karlsruhe Institute of Technology (KIT), Engesserstraße 15, D-76131 Karlsruhe (Germany), E-mail: claus.feldmann@kit.edu

SUPPORTING INFORMATION (SI)

Content

1. Analytical Techniques

X-ray powder diffraction (XRD). X-ray powder diffraction analysis was performed with a STOE Stadi-P diffractometer using Cu-$K_{\alpha 1}$ ($\lambda = 154.06$ pm) radiation with a Ge-monochromator. Rietveld refinements were performed with the program TOPAS-Academic (Version 5), using the *cif*-data to calculate the theoretical diffractogram.

Fourier-transformed infrared (FT-IR) spectra were recorded on a Bruker Vertex 70 FT-IR spectrometer (Bruker). The samples were measured as pellets in KBr. Thus, 300 mg of dried KBr and 0.5-1.0 mg of the sample were carefully pestled and pressed to a thin pellet.

Thermogravimetry (TG) and *differential thermal analysis (DTA)* were carried out with a Netzsch STA 449 F3 Jupiter device, using α-Al_2O_3 as crucible material and reference. Buoyancy effects were corrected by baseline subtraction of a blank measurement. The samples were measured under dried nitrogen up to 1000 °C with a heating rate of 10 K/min. The reaction gas was analyzed via IR-coupling by a Bruker Vertex 70 FT-IR spectrometer (Bruker). The Netzsch software PROTEUS Thermal Analysis (Version 5.2.1) was used for graphical illustration.

2. X-ray powder diffraction and Rietveld refinement

To verify composition and purity of the title compounds, X-ray powder diffraction (XRD) with Rietveld analysis was performed (Figure S1). Here, we have focused on the compounds with novel oxychloridoselenite(IV) anions. This includes [BMIm][$Se_4Cl_{15}O$] (**2**), [BMIm]$_2$[$Se_4Cl_{14}O_2$] (**3**), [BMPyr]$_2$[$Se_4Cl_{14}O_2$] (**4**), [BMPyr]$_2$[$Se_6Cl_{18}O_4$] (**5**) and [BMPyr]$_2$[$Se_6Cl_{14}O_6$] (**8**). [BMIm][Se_3Cl_{13}] (**1**), [BMIm]$_2$[$SeCl_4O$] (**6**) and [BMPyr]$_2$[$Se_2Cl_6O_2$] (**7**) with already known structural building units were not examined in detail. The comparison of the experimental powder diffractograms with the results of the respective Rietveld refinement (using the data of the single-crystal structure analysis as starting model for Rietveld refinement) shows good agreement for all compounds (Figure S1). Composition and structure of the title compounds were further confirmed by single-crystal structure analysis as well as by Fourier-transform infrared (FT-IR) spectroscopy and thermogravimetry (TG).

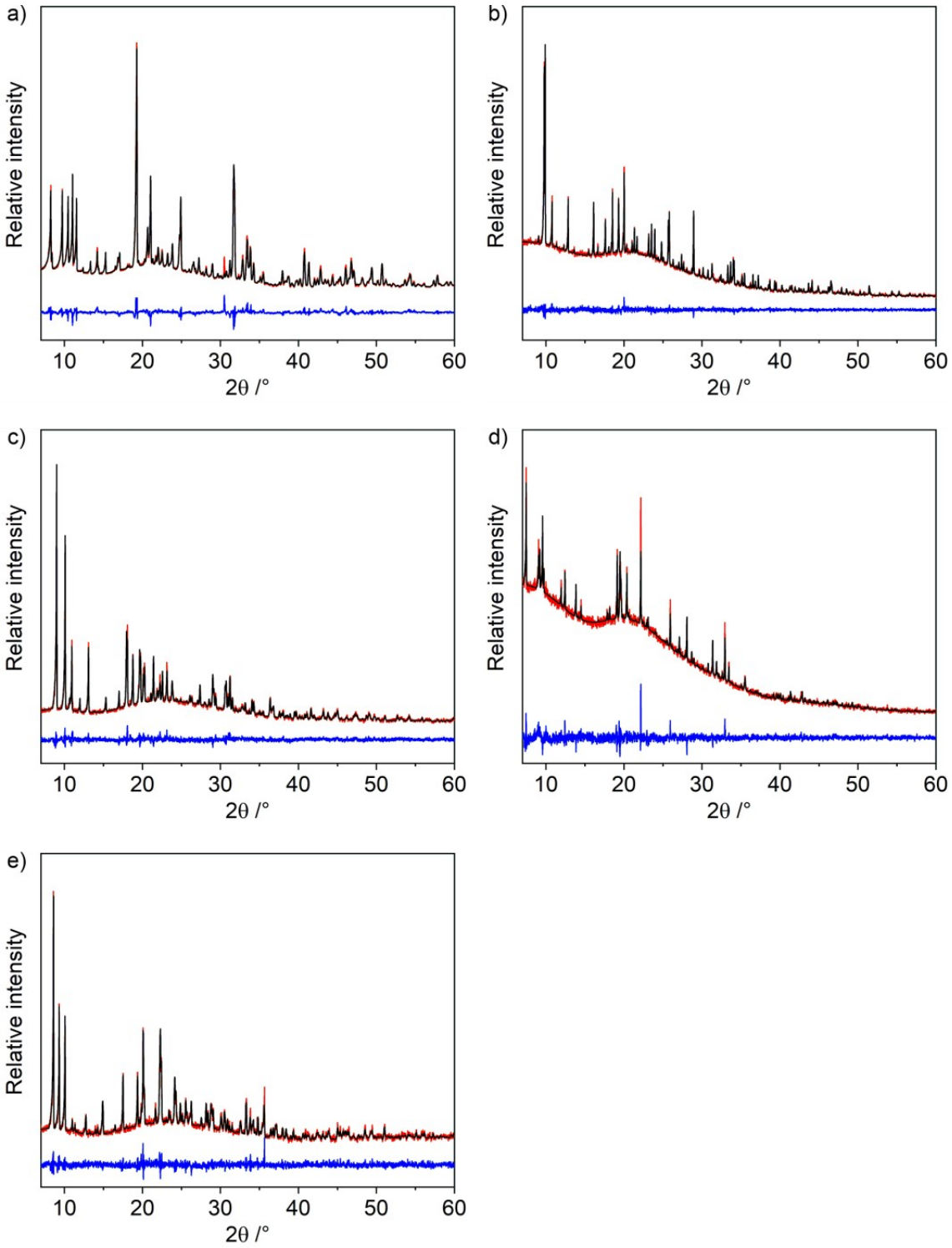

Figure S1. XRD and Rietveld analysis of a) [BMIm][$Se_4Cl_{15}O$] (**2**), b) [BMIm]$_2$[$Se_4Cl_{14}O_2$] (**3**), c) [BMPyr]$_2$[$Se_4Cl_{14}O_2$] (**4**), d) [BMPyr]$_2$[$Se_6Cl_{18}O_4$] (**5**) and e) [BMPyr]$_2$[$Se_6Cl_{14}O_6$] (**8**).

2. Crystal Structures

The crystallographic data and refinement details of the title compounds are listed in Table S1. The unit cells of **1-8** are displayed in Figures S2-S11. Figure S6 shows the hydrogen bonding with C–H···O distances < 280 pm between cation and anion for the compounds **3** and **4**. Figure S9 shows a (2×2×2) supercell of **6** illustrating the unidirectional alignment of the $[SeCl_4O]^{2-}$ anions.

Table S1. Crystallographic data and refinement details of [BMIm][Se_3Cl_{13}] (**1**), [BMIm][$Se_4Cl_{15}O$] (**2**), [BMIm]$_2$[$Se_4Cl_{14}O_2$] (**3**), [BMPyr]$_2$[$Se_4Cl_{14}O_2$] (**4**), [BMPyr]$_2$[$Se_6Cl_{18}O_4$] (**5**), [BMIm]$_2$[$SeCl_4O$] (**6**), [BMPyr]$_2$[$Se_2Cl_6O_2$] (**7**) and [BMPyr]$_2$[$Se_6Cl_{14}O_6$] (**8**).

Compound	**1**	**2**	**3**	**4**	**5**	**6**	**7**	**8**
W ($g \cdot mol^{-1}$)	837.0	1002.8	1122.6	1128.7	1460.4	515.2	687.1	1350.6
Space group	$P2_1$	*Pbca*	$P2_1/n$	$P2_1/n$	*P*-1	*P*1	*P*-1	$P2_1/n$
Flack parameter	0.00(2)	-	-	-	-	0.40(3)	-	-
a (pm)	840.5(1)	1675.7(1)	1140.1(1)	1042.0(2)	997.8(2)	857.0(4)	897.2(3)	1094.6(1)
b (pm)	1664.9(2)	2124.6(1)	1062.3(1)	1606.7(4)	1055.8(2)	885.7(4)	967.5(3)	1495.7(2)
c (pm)	975.2(1)	1690.6(1)	1619.5(2)	1237.3(2)	1380.1(2)	922.8(4)	1087.8(3)	1403.5(1)
α (°)	90	90	90	90	67.3(1)	73.7(1)	68.5(1)	90
β (°)	105.7(1)	90	94.7(1)	94.4(1)	68.6(1)	72.7(1)	66.8(1)	101.4(1)
γ (°)	90	90	90	90	87.3(1)	63.6(1)	66.6(1)	90
V (10^6 pm^3)	1313.6(3)	6018.7(6)	1954.7(4)	2065.3(7)	1240.9(4)	589.9(5)	771.7(4)	2252.4(4)
Z	2	8	2	2	1	1	1	2
$\rho_{calc.}$($g \cdot cm^{-3}$)	2.116	2.213	1.907	1.815	1.954	1.450	1.479	1.991
μ (mm^{-1})	5.524	12.135	4.735	4.481	5.421	2.057	2.932	5.738
λ(Mo-K_α) (pm)	71.073	134.143	71.073	71.073	71.073	71.073	71.073	71.073
T (K)	213	150	213	213	213	213	213	213
Observed reflections	4606	7215	3448	3623	4311	3970	2683	3949
Independent reflections	3735	5651	2315	1962	3216	1406	1993	2971
R_1 ($I \geq 2\sigma_I$)	0.0422	0.0240	0.0382	0.0366	0.0266	0.0404	0.0417	0.0229
R_1 (all data)	0.0604	0.0337	0.0516	0.0643	0.0414	0.1160	0.0545	0.0314
wR_2 ($I \geq 2\sigma_I$)	0.0892	0.0583	0.0845	0.0775	0.0598	0.0728	0.1071	0.0508
wR_2 (all data)	0.0981	0.0603	0.0864	0.0809	0.0628	0.0867	0.1176	0.0515
GooF	0.980	0.934	0.823	0.742	0.911	0.631	0.978	0.826

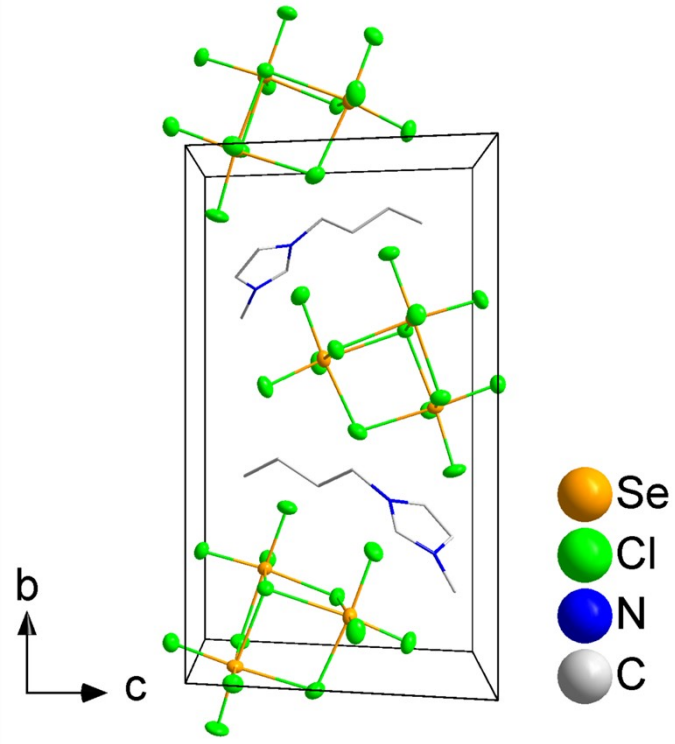

Figure S2. Unit cell of [BMIm][Se_3Cl_{13}] (**1**) (hydrogen atoms not shown for clarity).

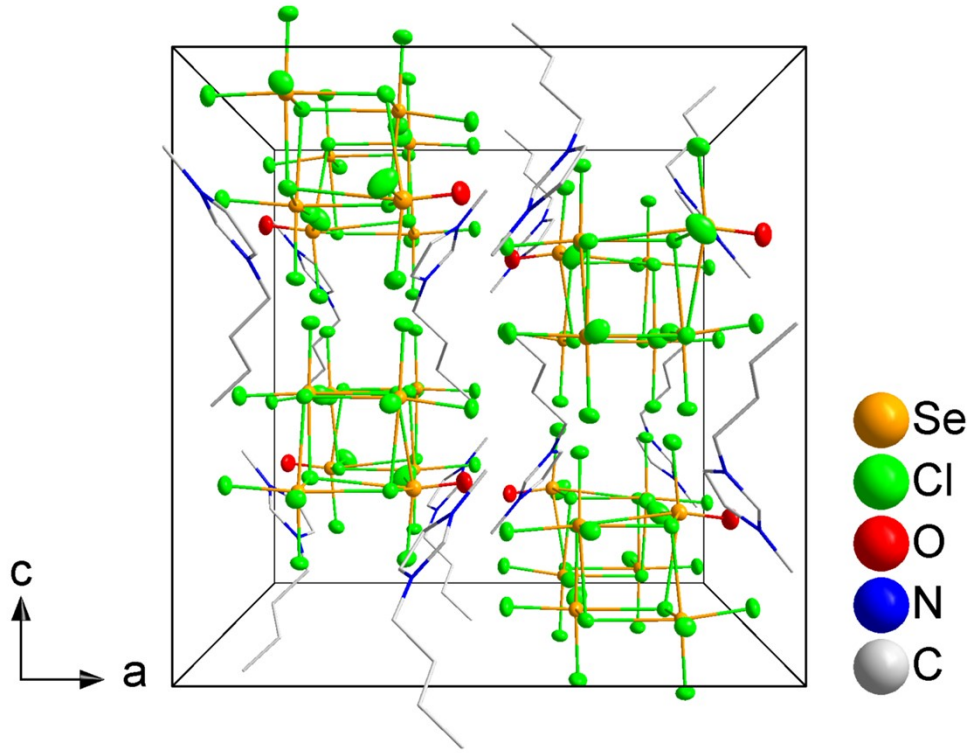

Figure S3. Unit cell of [BMIm][$Se_4Cl_{15}O$] (**2**) (hydrogen atoms not shown for clarity).

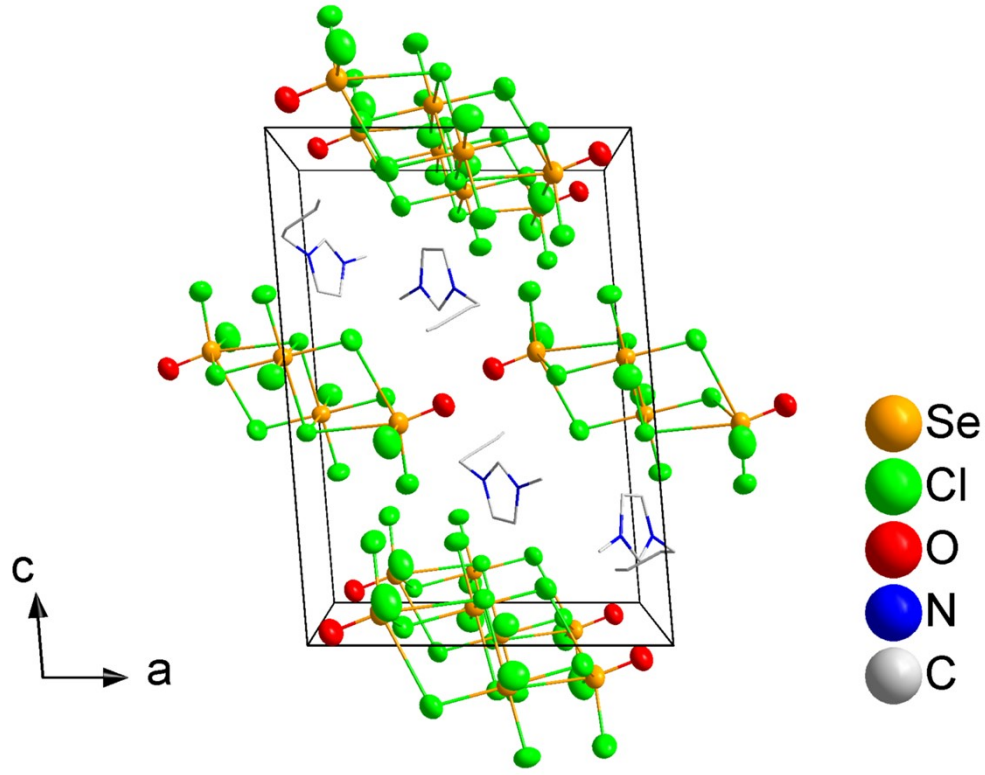

Figure S4. Unit cell of $[BMIm]_2[Se_4Cl_{14}O_2]$ (**3**) (hydrogen atoms not shown for clarity).

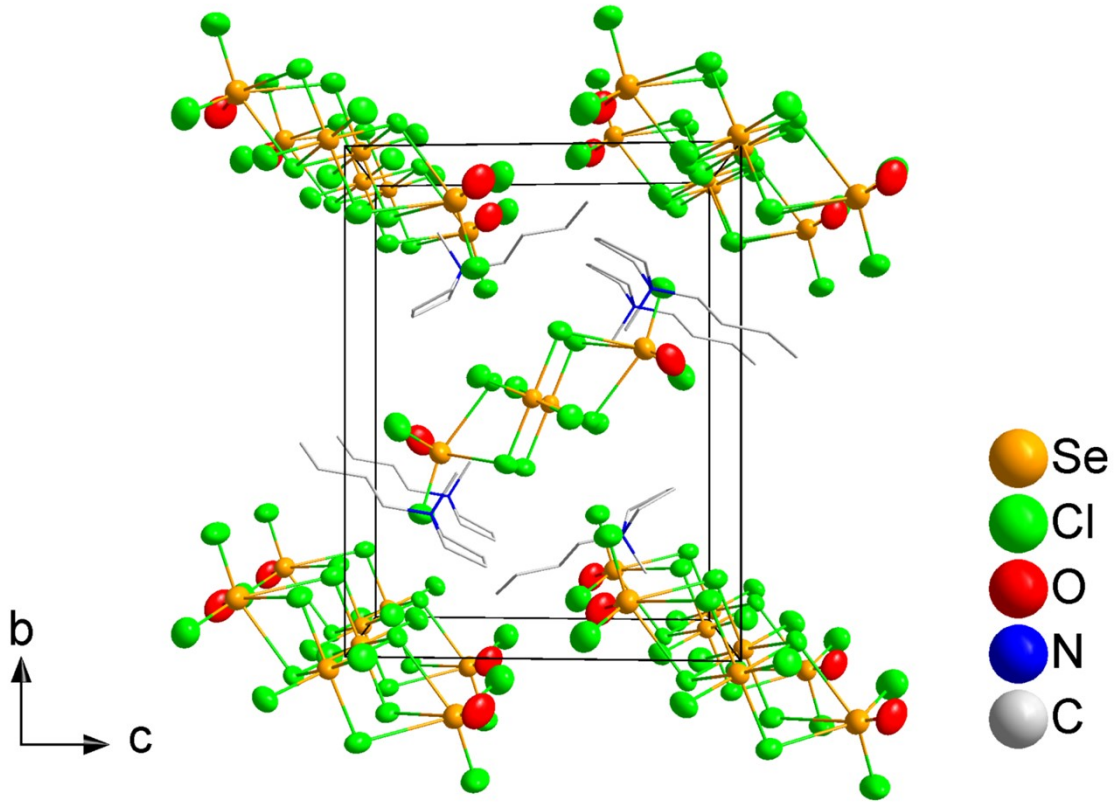

Figure S5. Unit cell of $[BMPyr]_2[Se_4Cl_{14}O_2]$ (**4**) (hydrogen atoms not shown for clarity).

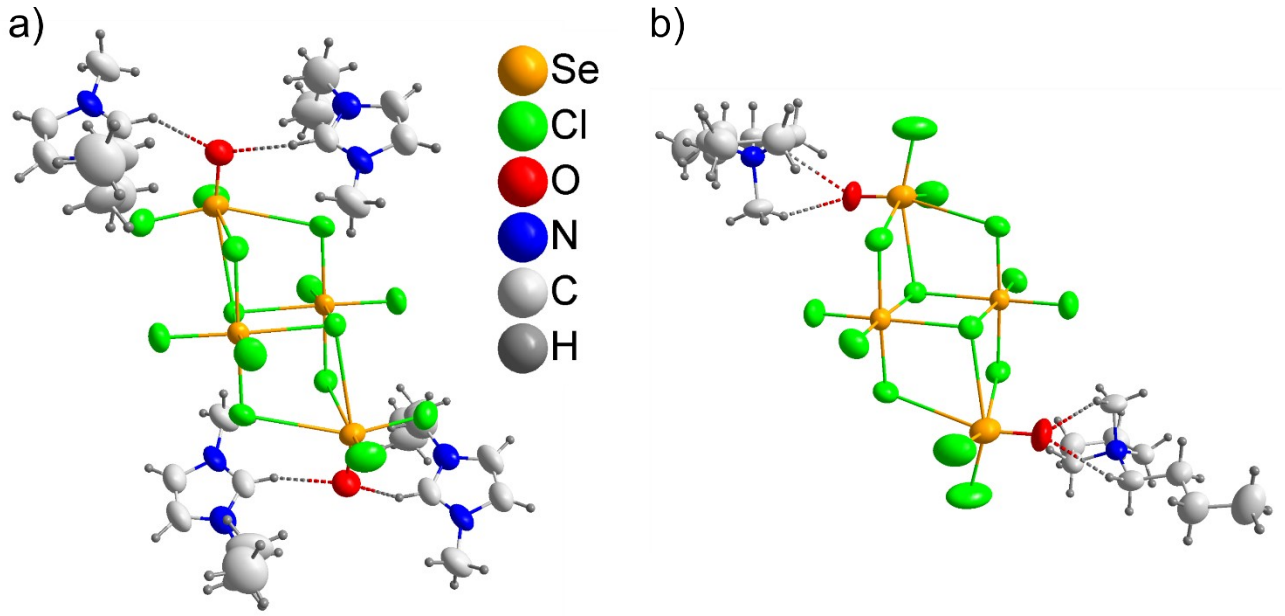

Figure S6. Hydrogen bonding with C–H···O distances < 280 pm between cation and anion in (a) compound **3** and (b) compound **4**.

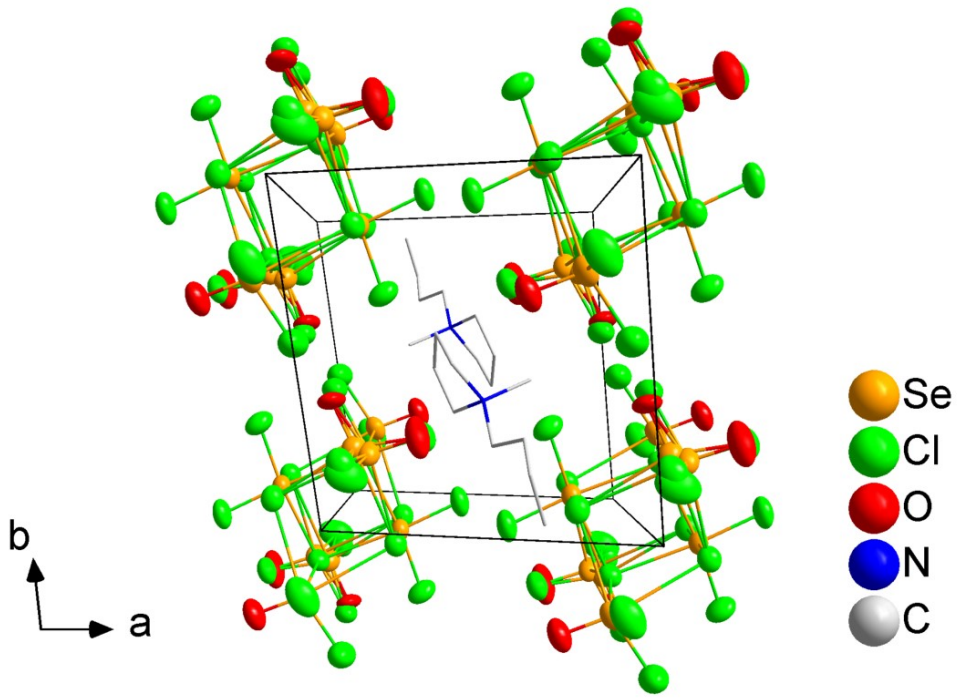

Figure S7. Unit cell of $[BMPyr]_2[Se_6Cl_{18}O_4]$ (**5**) (hydrogen atoms not shown for clarity).

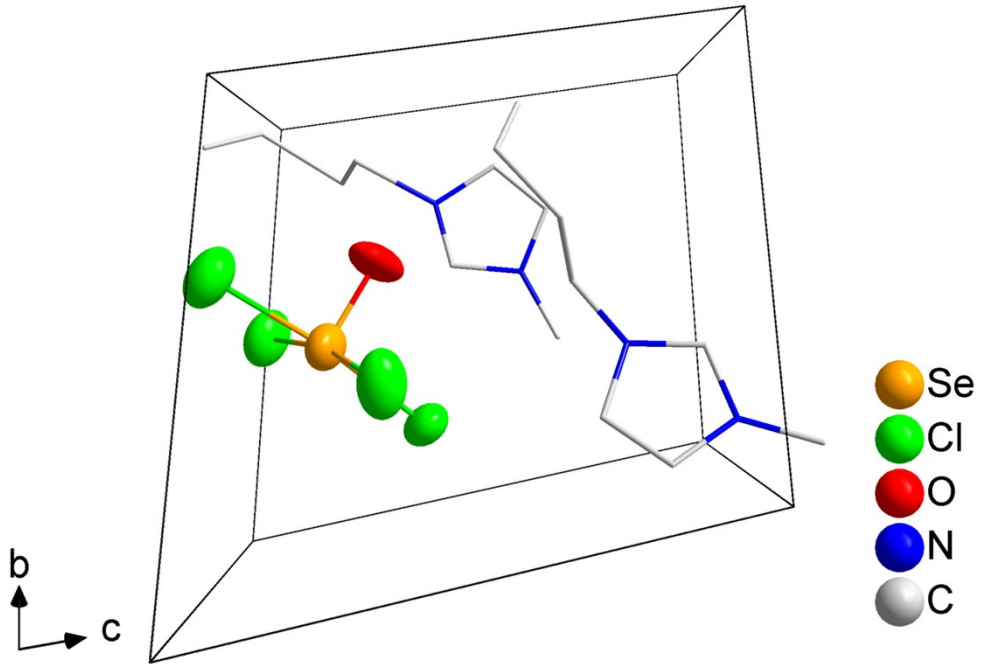

Figure S8. Unit cell of $[BMIm]_2[SeCl_4O]$ (**6**) (hydrogen atoms not shown for clarity).

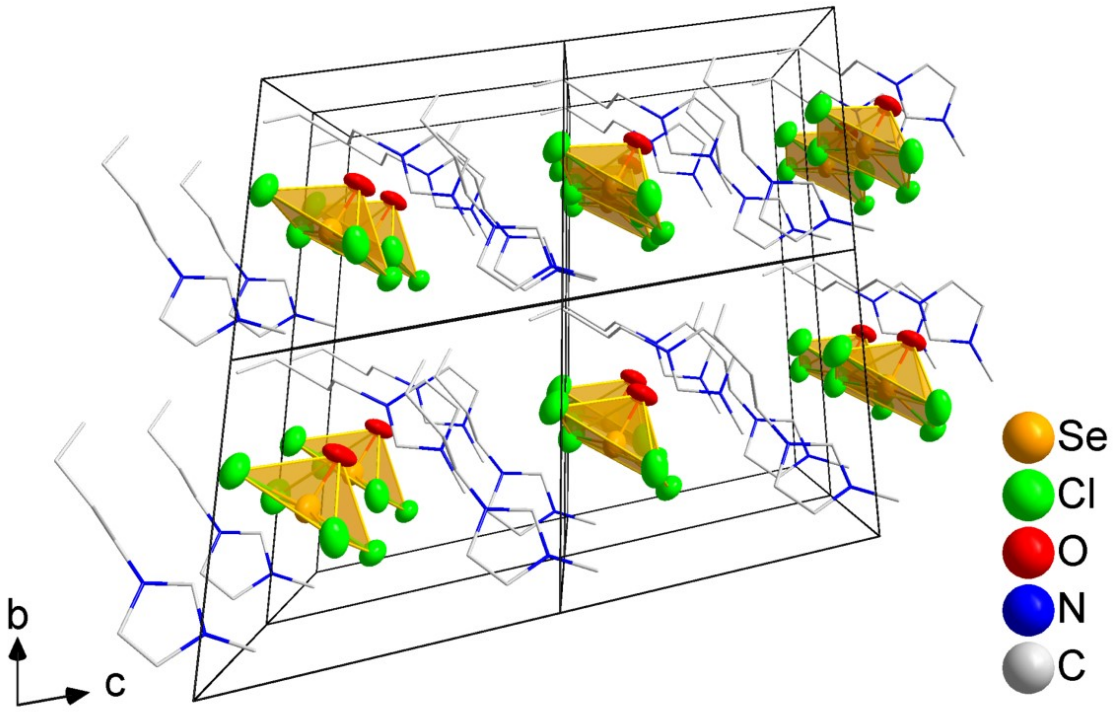

Figure S9. (2×2×2) Supercell of $[BMIm]_2[SeCl_4O]$ (**6**) (hydrogen atoms not shown for clarity).

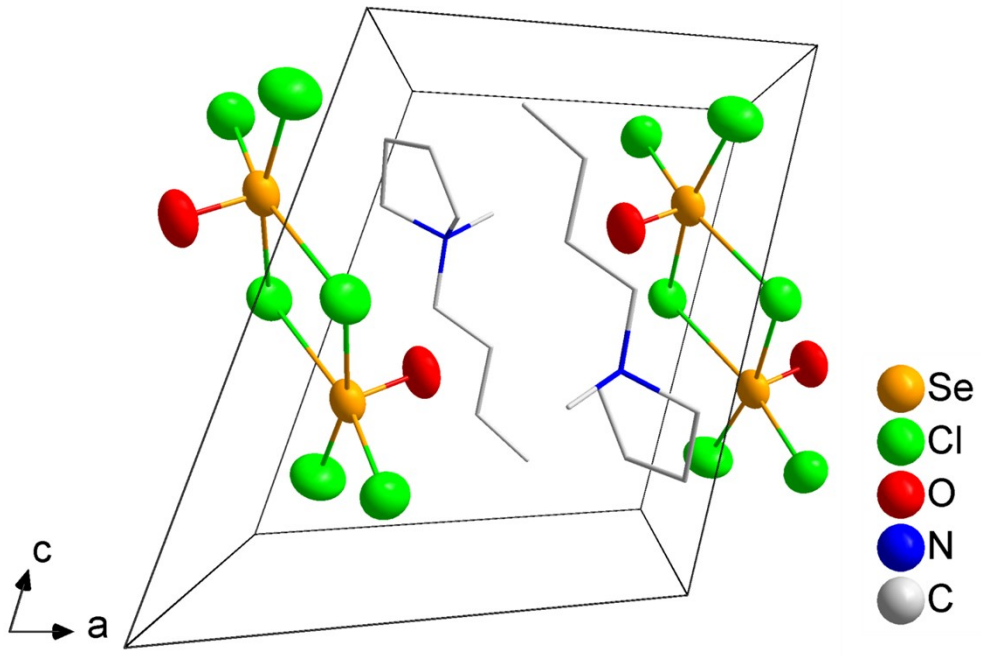

Figure S10. Unit cell of $[BMPyr]_2[Se_2Cl_6O_2]$ (**7**) (hydrogen atoms not shown for clarity).

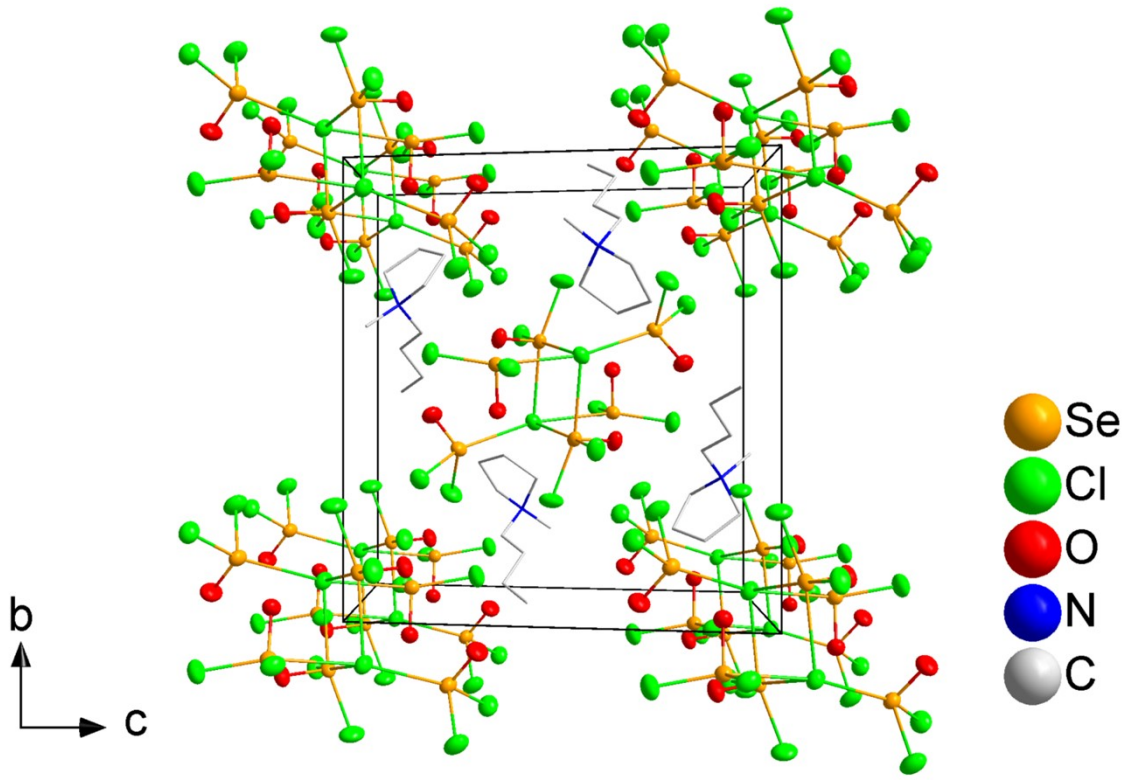

Figure S11. Unit cell of $[BMPyr]_2[Se_6Cl_{14}O_6]$ (**8**) (hydrogen atoms not shown for clarity).

4. Thermal Analysis

Thermal analysis with thermogravimetry (TG, Figure S12) and differential thermal analysis (DTA, Figure S13) show the thermal properties of the compounds **2-5** and **8**. This includes a two-step decomposition as well as the melting points of **3**, **4**, **5** at 70-80 °C. A quantification of the thermal decomposition also allows to validate the chemical composition and purity of the title compounds (*see main paper: Table 5*).

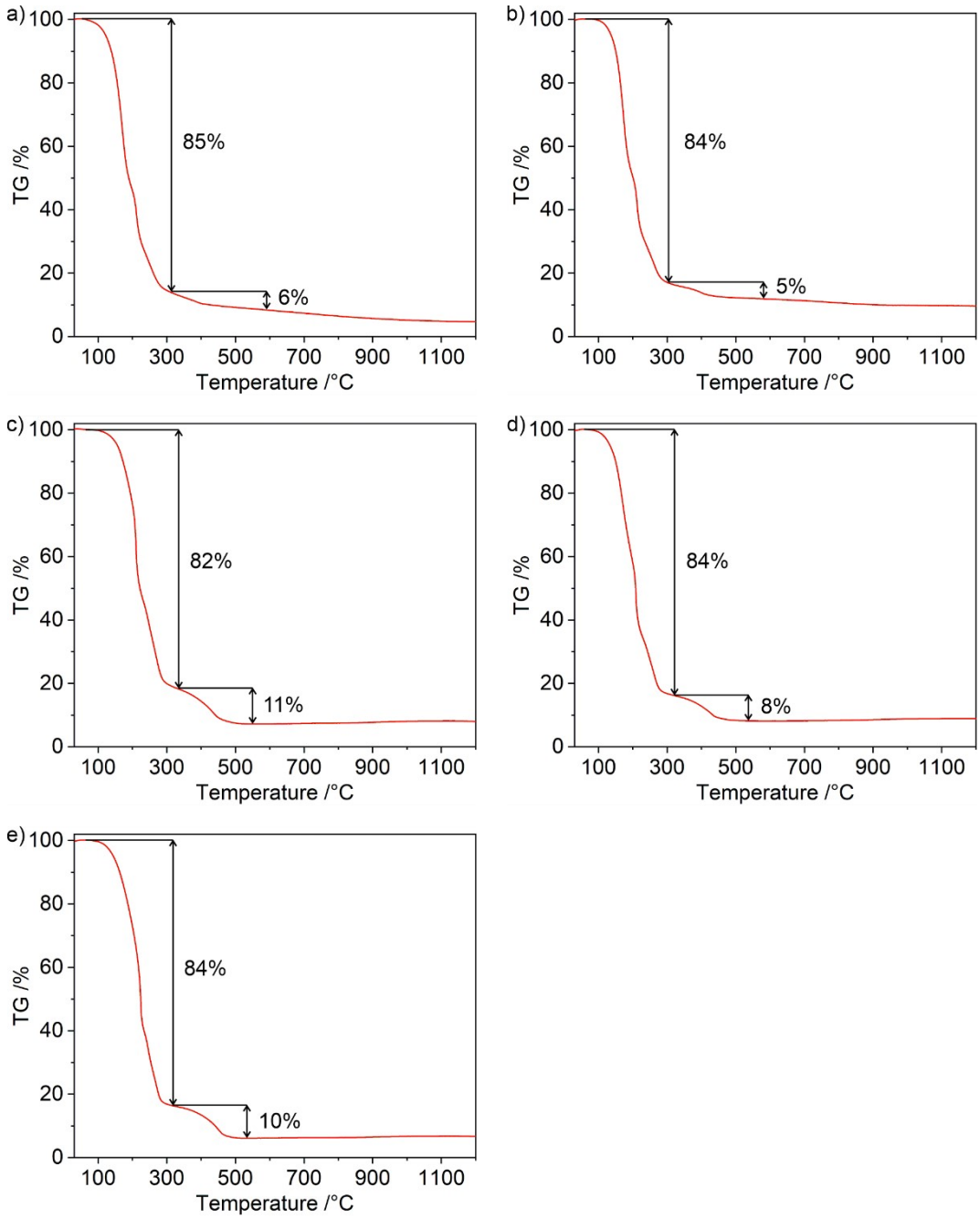

Figure S12. TG analysis of a) [BMIm][$Se_4Cl_{15}O$] (**2**), b) [BMIm]$_2$[$Se_4Cl_{14}O_2$] (**3**), c) [BMPyr]$_2$[$Se_4Cl_{14}O_2$] (**4**), d) [BMPyr]$_2$[$Se_6Cl_{18}O_4$] (**5**) and e) [BMPyr]$_2$[$Se_6Cl_{14}O_6$] (**8**).

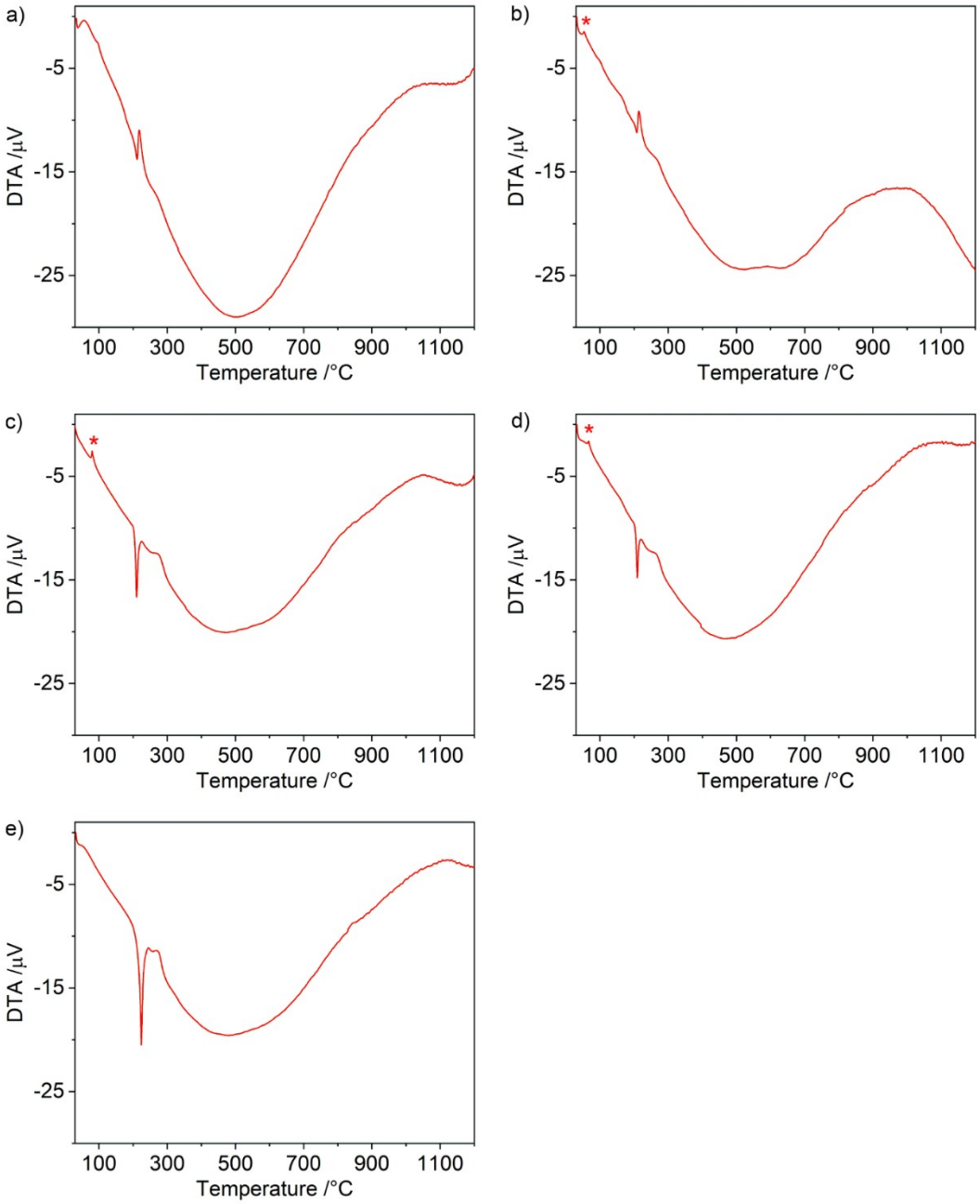

Figure S13. DTA analysis of a) [BMIm][$Se_4Cl_{15}O$] (**2**), b) [BMIm]$_2$[$Se_4Cl_{14}O_2$] (**3**), c) [BMPyr]$_2$[$Se_4Cl_{14}O_2$] (**4**), d) [BMPyr]$_2$[$Se_6Cl_{18}O_4$] (**5**) and e) [BMPyr]$_2$[$Se_6Cl_{14}O_6$] (**8**) with the melting point for **3**, **4**, **5** indicated by *.